

Electronic Supplementary Information (ESI) for:

A chiral mixed metal-organic framework based on Ni(saldpen)

metalloligand: synthesis, characterization and catalytic performances

Yanwei Ren, Xiaofei Cheng, Shaorong Yang, Chaorong Qi, Huanfeng Jiang* and Qiuping Mao

School of Chemistry and Chemical Engineering, South China University of Technology, Guangzhou, 510640, China.

E-mail: jianghf@scut.edu.cn

1. Table S1. Selected bond lengths [\AA] and angles [$^\circ$] for 1	2
2. Fig. S1. ^1H NMR spectrum of ligand H_4L	4
3. Fig. S2. ^{13}C NMR spectrum of ligand H_4L	4
4. Fig. S3. IR spectrum of $\text{Ni-H}_2\text{L}$	5
5. Fig. S4. IR spectrum of CMOF 1	5
6. Fig. S5. UV-vis spectrum of $\text{Ni-H}_2\text{L}$	6
7. Fig. S6. Space-filling model of 1 as viewed along the <i>b</i> -axis.....	6
8. Fig. S7. Thermogravimetric analysis (TGA) curve for 1	7
9. Fig. S8. GC of racemic PC.....	7
10. Fig. S9. GC of PC catalyzed by CMOF 1 and NBu_4Br (Table 1, entry 3)	8
11. Fig. S10. The influence of the reaction time on the conversion of PO.....	8

Table S1. Selected bond lengths [\AA] and angles [$^\circ$] for compound **1**

Bond lengths			
Cd(2)-O(15)	2.241(7)	Cd(4)-O(12)	2.189(9)
Cd(2)-O(7)	2.258(8)	Cd(4)-O(5W)	2.316(10)
Cd(2)-O(2W)	2.291(8)	Cd(4)-O(22)	2.412(9)
Cd(2)-O(4)	2.321(7)	Cd(4)-O(4W)	2.59(2)
Cd(2)-O(3)	2.400(8)	Ni(2)-N(3)	1.815(7)
Cd(2)-Cl(1)	2.514(3)	Ni(2)-N(4)	1.829(7)
Cd(3)-O(8)	2.208(8)	Ni(2)-O(5)	1.832(6)
Cd(3)-O(11)	2.215(7)	Ni(2)-O(6)	1.866(6)
Cd(3)-O(24)	2.229(8)	Ni(1)-N(2)	1.820(8)
Cd(3)-O(25)	2.460(10)	Ni(1)-N(1)	1.832(7)
Cd(3)-O(3W)	2.480(14)	Ni(1)-O(2)	1.823(7)
Cd(3)-O(23)	2.613(9)	Ni(1)-O(1)	1.870(6)
Cd(3)-O(7)	2.643(7)	Ni(3)-O(9)	1.839(6)
Cd(1)-O(16)	2.195(7)	Ni(3)-N(5)	1.853(8)
Cd(1)-O(19)	2.291(8)	Ni(3)-N(6)	1.858(8)
Cd(1)-O(1W)	2.267(7)	Ni(3)-O(10)	1.860(6)
Cd(1)-O(17)	2.351(8)	Ni(4)-O(13)	1.807(7)
Cd(1)-O(6W)	2.378(13)	Ni(4)-N(8)	1.833(8)
Cd(1)-Cl(1)	2.603(4)	Ni(4)-O(14)	1.840(7)
Cd(4)-O(21)	2.122(9)	Ni(4)-N(7)	1.831(9)
Cd(4)-O(23)	2.138(7)		
Bond angles			
O(15)-Cd(2)-O(7)	173.1(3)	O(16)-Cd(1)-O(17)	88.3(3)
O(15)-Cd(2)-O(2W)	96.4(3)	O(19)-Cd(1)-O(17)	81.8(3)
O(7)-Cd(2)-O(2W)	78.5(3)	O(1W)-Cd(1)-O(17)	165.9(3)
O(15)-Cd(2)-O(4)	87.3(3)	O(16)-Cd(1)-O(6W)	91.7(4)
O(7)-Cd(2)-O(4)	99.4(3)	O(19)-Cd(1)-O(6W)	83.9(4)
O(2W)-Cd(2)-O(4)	149.0(3)	O(1W)-Cd(1)-O(6W)	84.5(4)
O(15)-Cd(2)-O(3)	86.3(3)	O(17)-Cd(1)-O(6W)	88.3(4)
O(7)-Cd(2)-O(3)	98.6(3)	O(16)-Cd(1)-Cl(1)	93.3(2)
O(2W)-Cd(2)-O(3)	94.8(3)	O(19)-Cd(1)-Cl(1)	90.1(2)
O(4)-Cd(2)-O(3)	54.6(3)	O(1W)-Cd(1)-Cl(1)	100.0(2)
O(15)-Cd(2)-Cl(1)	90.5(2)	O(17)-Cd(1)-Cl(1)	85.9(2)
O(7)-Cd(2)-Cl(1)	86.6(2)	O(6W)-Cd(1)-Cl(1)	172.2(4)
O(2W)-Cd(2)-Cl(1)	107.1(3)	O(21)-Cd(4)-O(23)	167.6(4)
O(4)-Cd(2)-Cl(1)	103.6(2)	O(21)-Cd(4)-O(12)	91.9(4)
O(3)-Cd(2)-Cl(1)	158.1(2)	O(23)-Cd(4)-O(12)	98.9(3)
O(8)-Cd(3)-O(11)	130.6(3)	O(21)-Cd(4)-O(5W)	100.6(4)
O(8)-Cd(3)-O(24)	82.0(3)	O(23)-Cd(4)-O(5W)	86.3(4)
O(11)-Cd(3)-O(24)	143.8(3)	O(12)-Cd(4)-O(5W)	86.1(4)
O(8)-Cd(3)-O(25)	86.8(4)	O(21)-Cd(4)-O(22)	56.3(3)

O(11)-Cd(3)-O(25)	78.6(3)	O(23)-Cd(4)-O(22)	112.4(3)
O(24)-Cd(3)-O(25)	89.9(4)	O(12)-Cd(4)-O(22)	147.9(3)
O(8)-Cd(3)-O(3W)	99.7(4)	O(5W)-Cd(4)-O(22)	102.8(4)
O(11)-Cd(3)-O(3W)	89.3(3)	O(21)-Cd(4)-O(4W)	91.8(5)
O(24)-Cd(3)-O(3W)	101.3(4)	O(23)-Cd(4)-O(4W)	83.9(4)
O(25)-Cd(3)-O(3W)	167.7(3)	O(12)-Cd(4)-O(4W)	81.1(5)
O(8)-Cd(3)-O(23)	132.2(3)	O(5W)-Cd(4)-O(4W)	162.5(6)
O(11)-Cd(3)-O(23)	96.3(2)	O(22)-Cd(4)-O(4W)	94.4(6)
O(24)-Cd(3)-O(23)	50.4(3)	O(16)-Cd(1)-O(17)	88.3(3)
O(25)-Cd(3)-O(23)	95.3(3)	O(24)-Cd(3)-O(7)	132.4(3)
O(8)-Cd(3)-O(23)	132.2(3)	O(25)-Cd(3)-O(7)	99.4(3)
O(11)-Cd(3)-O(23)	96.3(2)	O(3W)-Cd(3)-O(7)	76.8(4)
O(24)-Cd(3)-O(23)	50.4(3)	O(23)-Cd(3)-O(7)	165.0(3)
O(25)-Cd(3)-O(23)	95.3(3)	O(16)-Cd(1)-O(19)	169.3(3)
O(3W)-Cd(3)-O(23)	88.1(4)	O(16)-Cd(1)-O(1W)	103.9(3)
O(8)-Cd(3)-O(7)	52.5(3)	O(19)-Cd(1)-O(1W)	85.4(3)

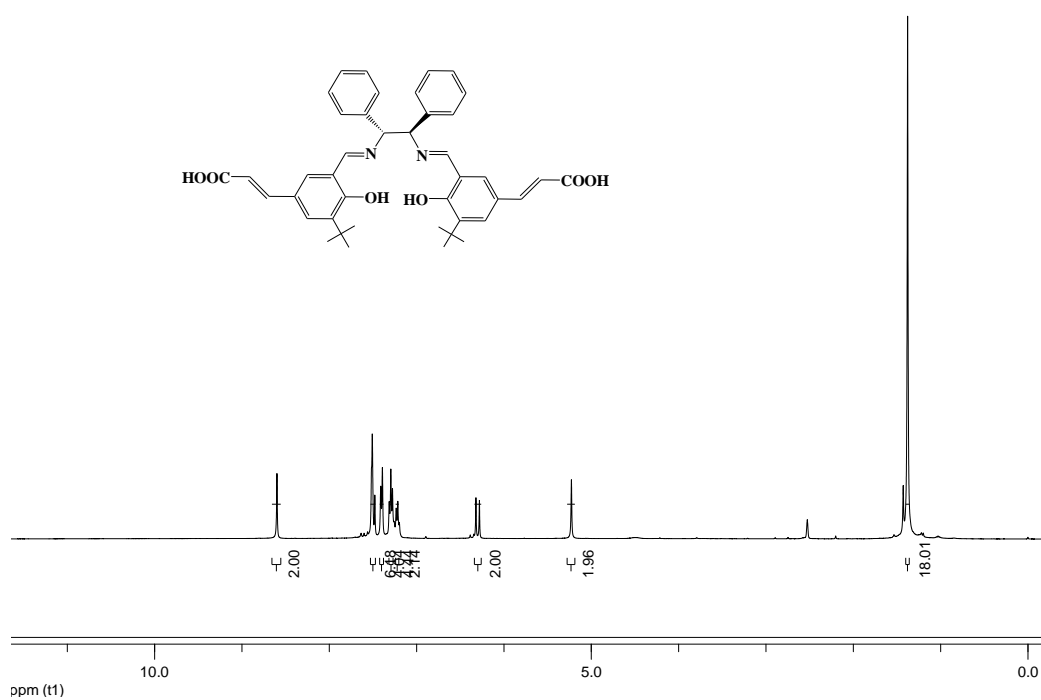


Fig. S1. ¹H NMR spectrum of ligand H₄L

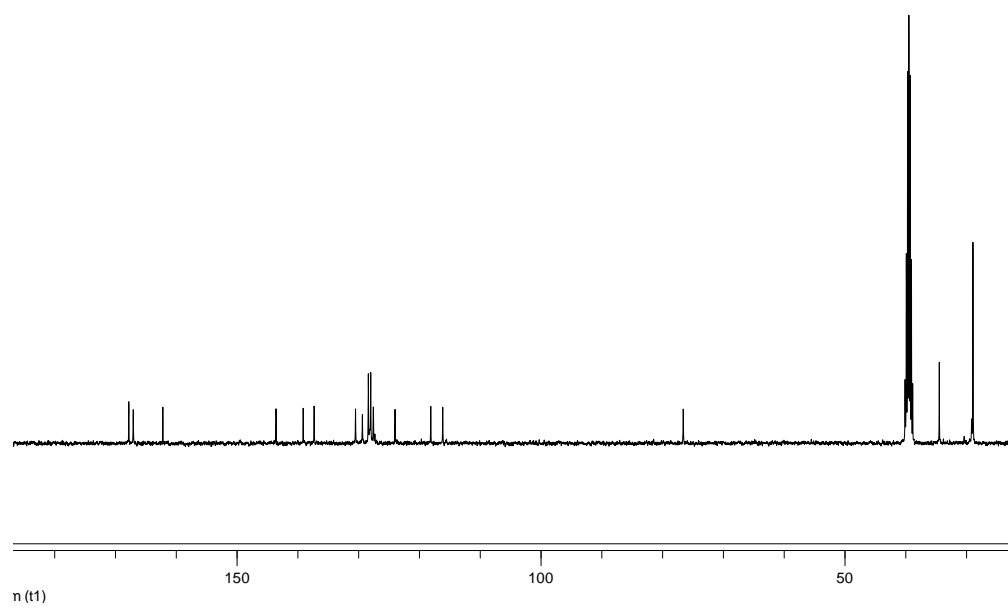


Fig. S2. ¹³C NMR spectrum of ligand H₄L

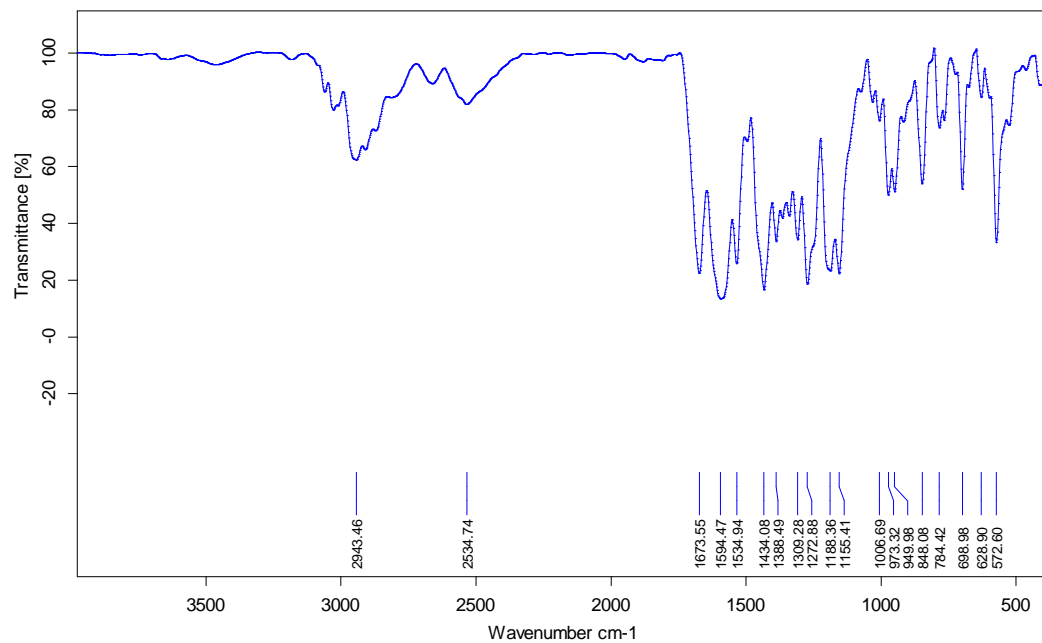


Fig. S3. IR spectrum of Ni-H₂L

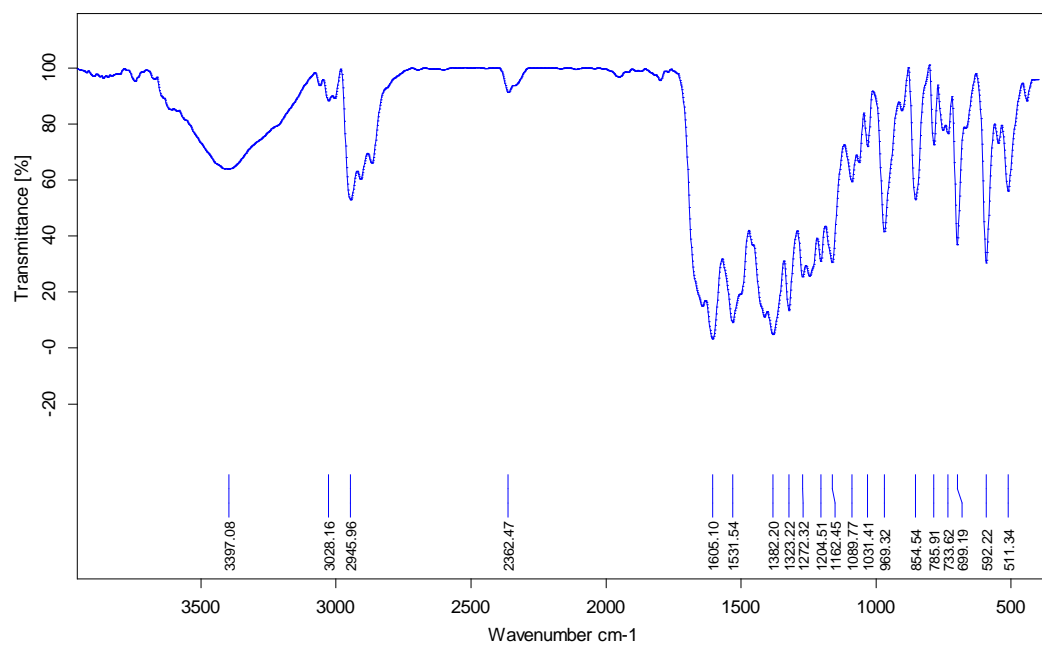


Fig. S4. IR spectrum of ligand CMOF 1

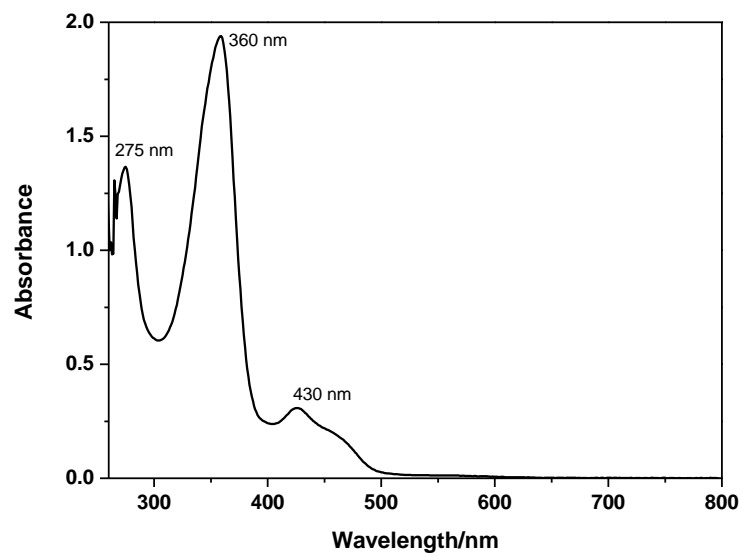


Fig. S5. UV-vis spectrum of Ni-H₂L

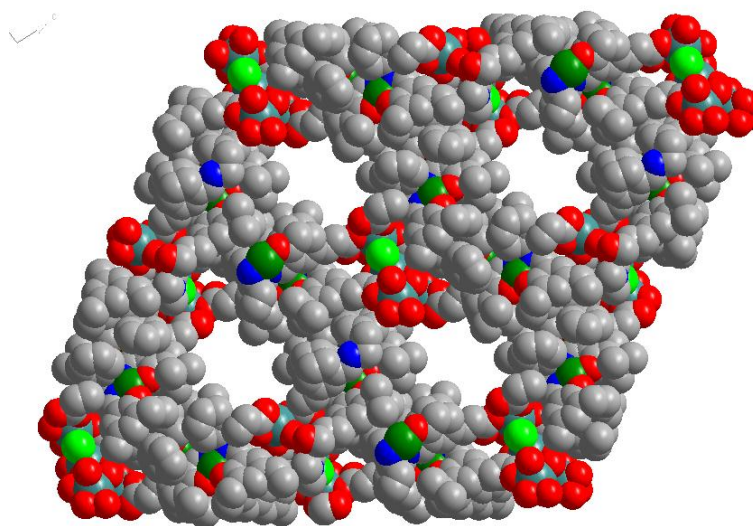


Fig. S6. Space-filling model of **1** as viewed along the *b*-axis.

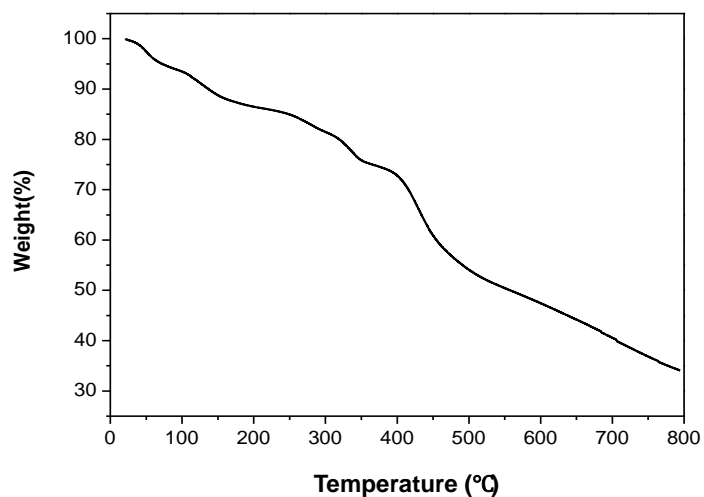
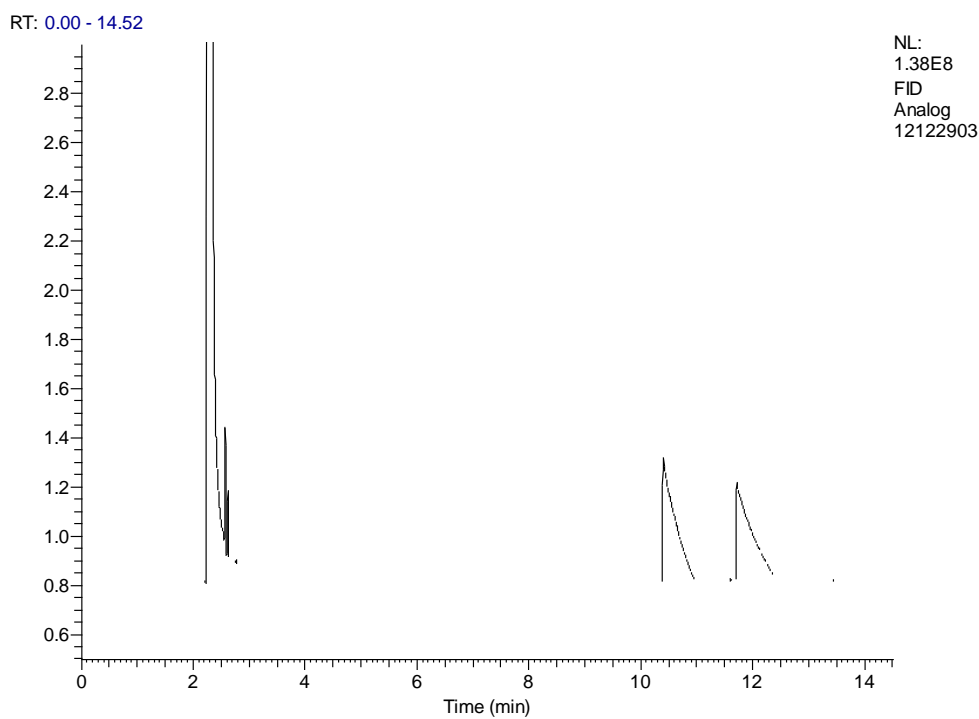


Fig. S7. TGA curve for **1**.



PEAK LIST

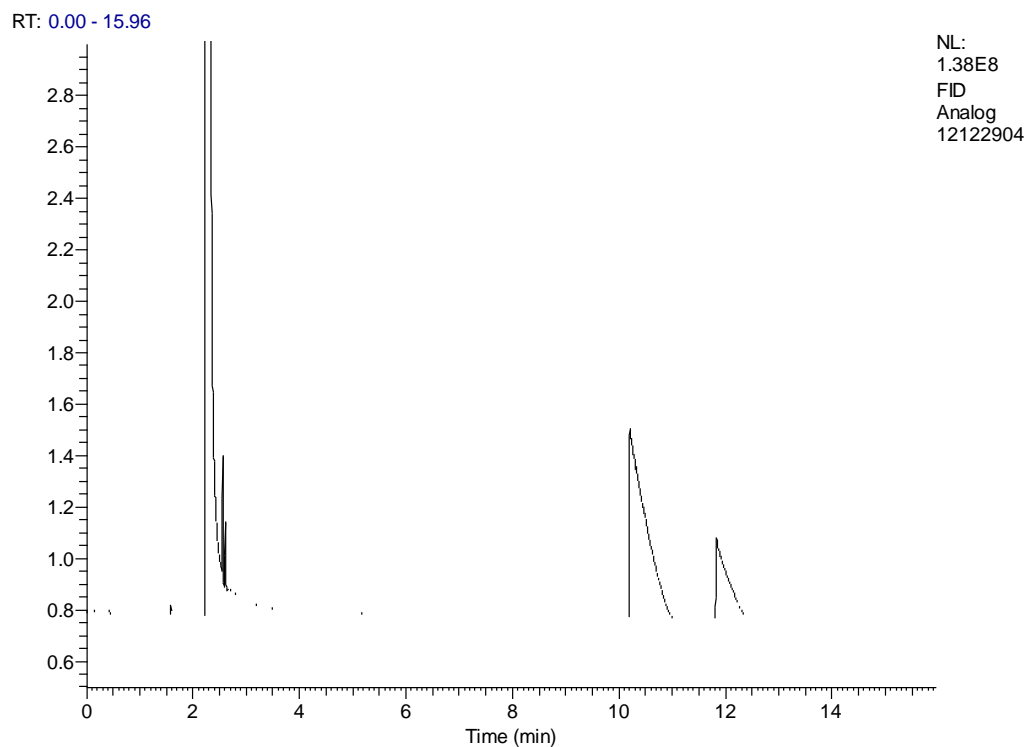
Ren01.raw

RT: 0.00 - 14.52

Number of detected peaks: 2

Apex	Start RT	End RT	Area	Area%	Height	% Height
10.40	10.34	10.97	10195313	50.46	692327.653	55.82
11.72	11.67	12.42	10009716	49.54	552982.694	44.18

Fig. S8. GC of racemic PC.



PEAK LIST

Ren02.raw

RT: 0.00 – 115.96

Number of detected peaks: 2

Apex	Start RT	End RT	Area	Area%	Height	% Height
10.2	10.19	11.01	20249891	75.84	1012059	70.21
11.83	11.8	12.5	6449297	24.16	429470	29.79

Fig. S9. GC of PC catalyzed by CMOF **1** and NBu_4Br (Table 1, entry 3).

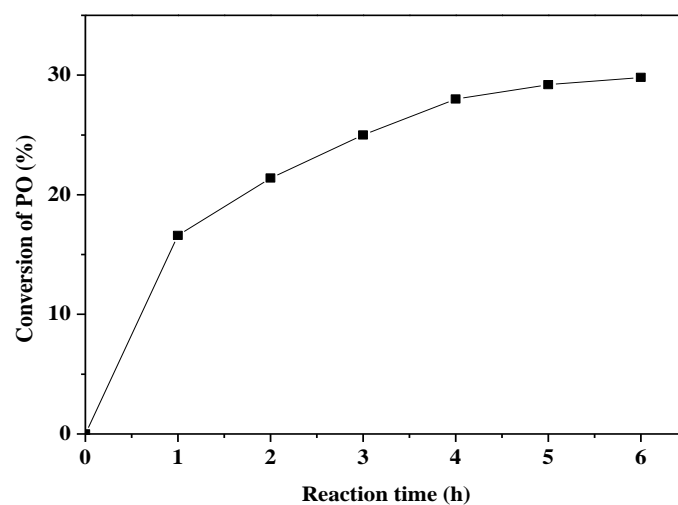


Fig. S10. The influence of the reaction time on the conversion of PO. Reaction conditions: PO (15 mmol), co-catalysts (2 mol %), catalyst (100 mg), CO_2 pressure (2 MPa), reaction temperature (25 °C).